Part I
The Distribution and Abundance of Planktonic Larval Stages of *Lepeophtheirus salmonis*: Surveillance and Modeling

Chapter 1
Modeling the Distribution and Abundance of Planktonic Larval Stages of *Lepeophtheirus salmonis* in Norway

Lars Asplin, Karin K. Boxaspen, and Anne D. Sandvik

Introduction

Norway spans from a latitude of 58° N to 71° N and has a long coastline of about 3000 km (Figure 1.1). The coast has numerous islands and fjords of various sizes, and the topography is frequently complicated. Some general features exist for the Norwegian fjords and usually they are much longer than they are wide. Fjord lengths can be several tens of kilometers, and the longest fjord, the Sognefjord, is more than 200 km long with a width between 2 and 5 km. Fjords are often several hundreds of meters deep, and deeper than the outside coastal ocean. Steep mountains surrounding the fjords influence the atmospheric conditions by channeling the winds along the fjord axis, which provides shelter and reduced possibilities for long wave fetches. The oceanography of fjords is complicated by winds, freshwater runoff, tides, and internal wave interaction with the coastal ocean (Farmer and Freeland 1983; Dyer 1997). The topography of the fjords further complicates the dynamics. For example, in a narrow fjord, less than about 1 km, the hydrodynamics will be unaffected by the rotation of the earth. In a fjord wider than 1–2 km, the earth's rotation hydrodynamics must be considered, and the difference between nonrotating and rotating dynamics is large. In nonrotating dynamics, the equilibrium state, or the path of least resistance, is one of stable water masses and no motion or surface elevation. In rotating dynamics, the rotation of the earth, the Coriolis acceleration, must be balanced by the other forces. The equilibrium state is one of motion, the geostrophic current, and horizontal pressure forces. In the rotating system, energy needs to be supplied to the water masses to slow them down toward a state of no motion. Interestingly, little is known about the transition between nonrotating and rotating dynamics.

The water masses are relatively cold and have strong upper layer stratification. Temperatures in the upper 10–20-m depths range between 0 and 5°C during winter and can exceed 20°C at the surface during summer. Below the pycnocline at 30–50-m depth, the mean temperature is between 7 and 8°C. Seasonal temperature variation is much lower, lagging temperatures in the surface layer by several months. This temperature range is favorable for the farming of Atlantic salmon. The water stratification is

Salmon Lice: An Integrated Approach to Understanding Parasite Abundance and Distribution, First Edition. Edited by Simon Jones and Richard Beamish.

P1: SFK/UKS P2: SFK
BLBS084-01 BLBS084-Beamish July 6, 2011 14:16 Trim: 244mm×172mm

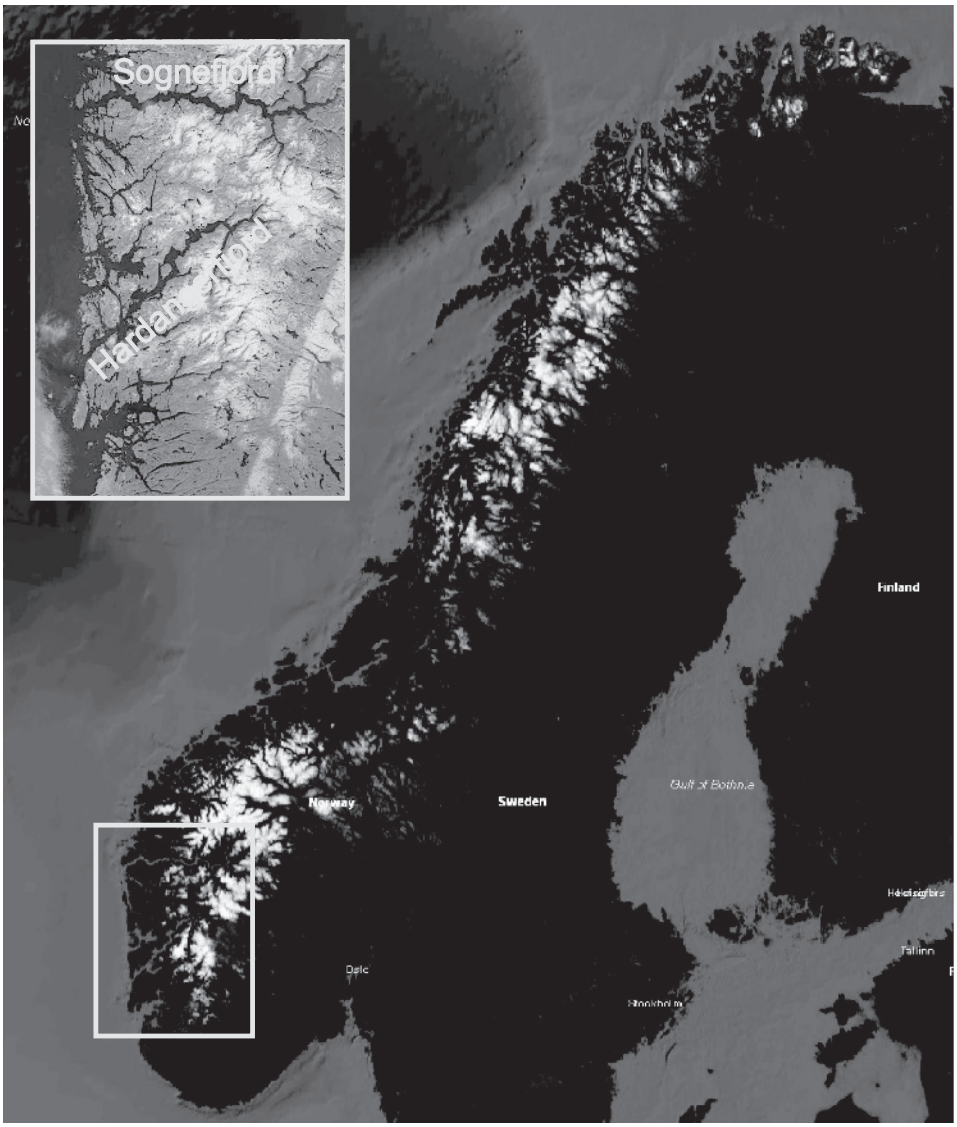

Figure 1.1. Norway with its 3000-km-long coastline and numerous fjords and islands suitable for fish farming. The two larger fjords, Hardangerfjord and Sognefjord, are shown inside the yellow square and the smaller picture. (See also color plate section.)

weakest during the cold season when the precipitation accumulates as snow in the mountains. During the spring and through to the end of the fall, river runoff and precipitation create a distinct surface brackish layer in the fjords. Such a layer is typically strongest in the inner part, as seen from a long section of hydrography in the Hardangerfjord from July 2008 (Figure 1.2). The brackish layer is gradually mixed with the deeper fjord water toward the coast. The brackish layer depth depends on the amount of discharged freshwater and fjord topography, and is typically between 1

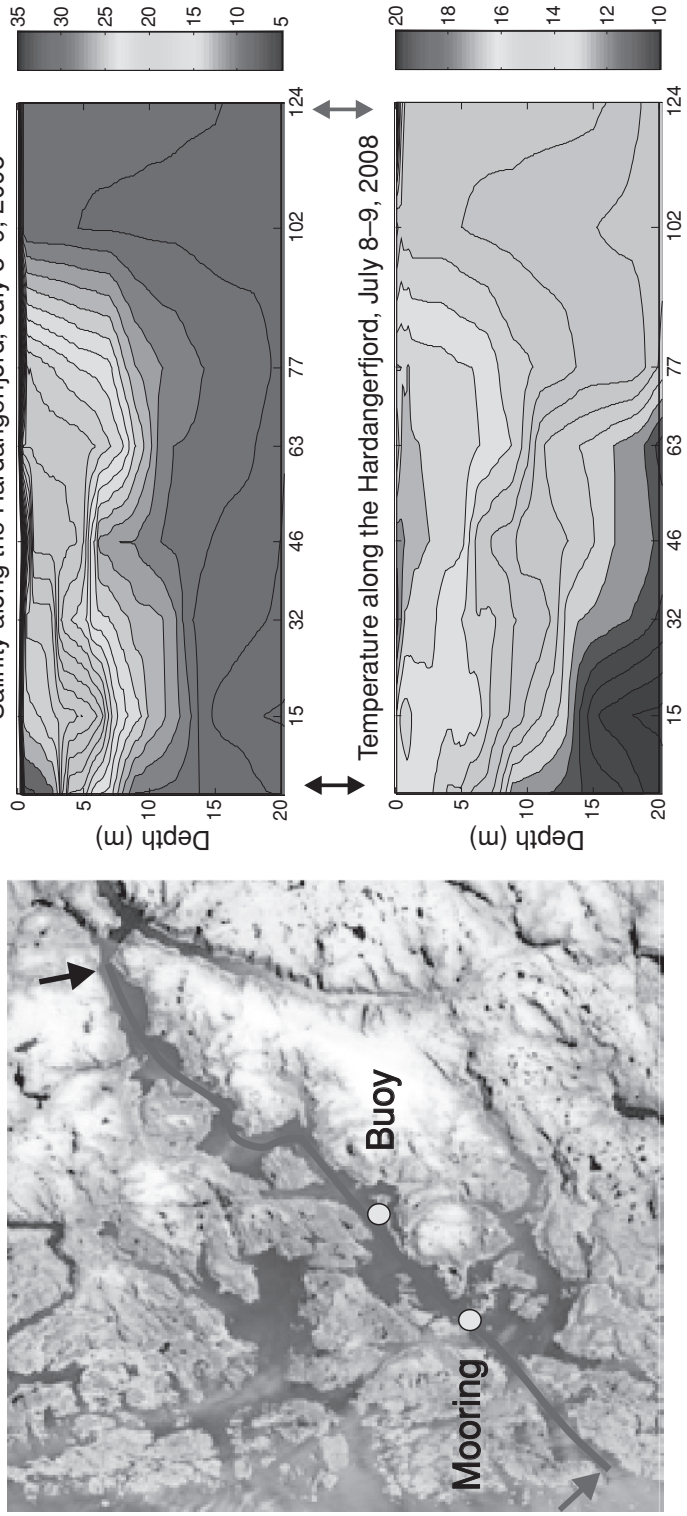

Figure 1.2. Vertical sections of salinity and temperature (°C) along the Hardangerfjord for a summer situation with a distinct brackish layer in the inner part of the fjord. The fjord mouth to the right on the figures is indicated by a red arrow on the map. The red line on the map marks the section and the black arrow the start of the section. The positions of an observational buoy and a current meter mooring are marked by yellow dots for later references. (See also color plate section.)

and 10 m for Norwegian fjords. The presence of the brackish layer, and the downward mixing of buoyant water, create a strong vertical gradient in temperature and salinity in the upper 10–20 m of the fjord water.

Many of the numerous rivers along the Norwegian coast contain Atlantic salmon and other salmonids. In an assessment report of a working group reporting to the Directorate for Nature Management, 452 salmon rivers were identified (Hansen et al. 2008). Almost half of these rivers have been negatively altered by human activities. The estimated number of wild Atlantic salmon returning from the ocean in 2007 was 470,000, which is the second lowest from 1983 to 2007 (Hansen et al. 2008).

Norwegian coastal waters and fjords are suitable for farming of Atlantic salmon not only due to the natural water quality conditions but also due to the large relatively sheltered areas. Since its beginning around 1970, salmon farming has increased enormously and today produces more than 800,000 tons (see Chapter 5 contributed by Ritchie and Boxaspen). This represents an abundance of approximately 300 million individuals in almost 1000 licensed sites (see also Chapter 5 contributed by Ritchie and Boxaspen; statistics from the Directorate of Fisheries, http://www.fdir.no). Thus, the number of farmed salmon is between 500 and 1000 times larger than that of the wild salmon. Just one licensed site potentially holds almost as many fish as the number of all wild stocks.

The salmon louse (*Lepeophtheirus salmonis*) is the main parasite on the Atlantic salmon in Norway. Salmon lice are mostly a threat to the welfare and existence of wild salmon stocks and are considered to be partly responsible for the observed wild stock decline (Hansen et al. 2008; Heuch et al. 2005). The salmon louse has ten stages, where the first three are planktonic (see the introductory chapter contributed by Hayward et al.). Environmental conditions of the water are critical for the growth and distribution of these planktonic stages.

The abundance and distribution of salmon lice in the fjord and coastal waters can be critical for the production of Atlantic salmon stocks. Strong variability of the environmental conditions will lead to variability of the abundance and distribution of the salmon lice in the fjord and coastal waters. Factors influencing this variability are the production of salmon lice eggs (mostly from the farmed fish; Heuch et al. 2005), the water current that determines the spreading of the planktonic salmon lice, the water temperature determining the growth rates of eggs and the larval stages, and the salinity influencing the salmon lice survival and behavior (Heuch 1995).

This chapter considers aspects of the salmon lice distribution and abundance in Norwegian fjord and coastal waters. Although we show results from two large fjord systems at the western coast, the Hardangerfjord and the Sognefjord, the results mostly apply to the whole Norwegian coast. We identify typical variability of the environmental conditions as current and hydrography and present model results and observations of salmon lice distribution. We do not consider production of lice from farms as a source of variability to planktonic salmon lice.

Methods to Determine Planktonic Louse Distribution and Abundance

A broad range of methods are needed for the collection of information that can be used to understand the dynamics of fjord areas. The spatial and temporal variability is sufficiently complex that there needs to be a massive observational system or a

combination of a few central observations and numerical modeling. Thus, we use a combined approach of both observations and numerical modeling as scientific methods. The use of numerical models has the extra advantage that the results can be used for hindcasts and forecasts, as well as to run applications such as the salmon lice growth and distribution model.

The numerical modeling approach we use is similar to models used in weather predictions. As we all know, the weather is a highly chaotic and a relatively unpredictable system on time scales more than a few days. The situation is slightly better in the ocean, as the evolution of the system is much slower and the predictable period longer. For weather predictions and ocean predictions, reliable results depend on a good initial state and, most importantly, on good forcing. Thus, we have spent much effort to optimize the forcing and have established an approach to simulate the spreading of the salmon lice. First, we needed detailed information of the winds and the atmospheric conditions to run a mesoscale atmospheric model. Second, we needed detailed information on the conditions in the coastal ocean outside the fjord to run a system consisting of an ocean and a nested coastal model. Then, we could run the fjord model and, finally, the salmon lice growth and advection model. Observations were needed for model validation and for the construction of initial model fields.

Quantifying the uncertainty of the model results identifies the limitations. However, this is not a trivial task, even with numerous observations. Dee (1995) describes a pragmatic approach to model validation. He proposed the following definition:

> Validation of a computational model is the process of formulating and substantiating explicit claims about the applicability and accuracy of computational results, with reference to the intended purpose of the model as well as to the natural system it represents.

Thus, a validated model is not necessarily "correct," but it has been subjected to a variety of validation activities that indicate the expected accuracy of model predictions. Model validation for generic numerical ocean models is an ongoing process. The described methods are generic in the sense that they can be applied to all areas of the Norwegian coast. Model implementations already exist for several fjord and coastal areas of Norway.

Observation of the Environmental Conditions

Measurements of salinity and temperature were made either with a CTD-sonde (SAIV SD204, http://www.saivas.no) or with sensors for conductivity and temperature from Aanderaa Instruments (http://www.aadi.no) attached to an observational buoy. Collectively, these instruments measure conductivity, temperature, and depth. The measuring interval of 1 second for the CTD-sonde was appropriate for making vertical profiles at various locations. The sensors of the observational buoy produced 10-minute averages of salinity, temperature, and density. Current measurements were made from either a vertical profiler, measuring flow in 1-m bins with a range of 30–50 m (the Nortek Aquadopp Profiler, http://www.nortek-as.com), or an Aanderaa Instruments Doppler current sensor 4100 (http://www.aadi.no) that measured the

P1: SFK/UKS P2: SFK
BLBS084-01 BLBS084-Beamish July 6, 2011 14:16 Trim: 244mm×172mm

current close to an observational buoy. The positions of the observational buoy and the current meter mooring are shown in Figure 1.2.

Observation of Salmon Lice—Sentinel Cages

Direct observations of free-living planktonic salmon lice stages are difficult. Some success has been achieved in Scottish lochs using a small plankton net (Penston et al. 2004). In Norwegian fjords, a similar approach has so far not experienced similar success. Instead, we have developed, over a 10-year period, an indirect method for assessing planktonic salmon lice abundance using small cages stocked with Atlantic salmon smolts as sentinels (see also Chapter 5 contributed by Ritchie and Boxaspen, and Chapter 2 contributed by Murray et al.). Each cage has a volume of approximately 1 m^3 holding 20–30 fish of 80–100 g (Figure 1.3). After 3-week deployment, the fish are recovered and the attached salmon lice are counted. We are working on an assessment of the accuracy of the sentinel cage method for estimating salmon lice infection and, especially, how to transfer these numbers to the infection pressure on the wild fish stock.

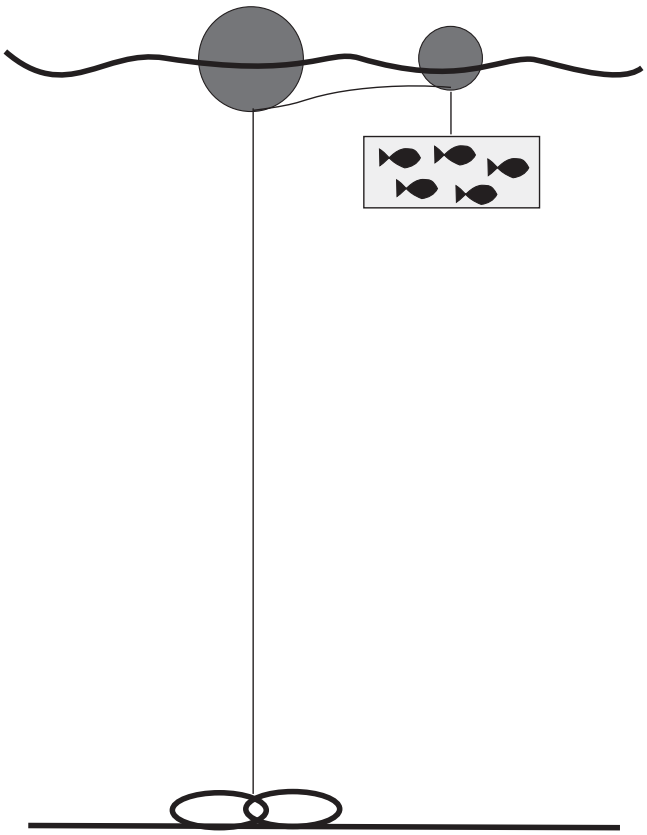

Figure 1.3. The layout of the sentinel cage being moored to a larger surface buoy attached to a ∼100-kg anchor. Typically, the moorings are deployed at depths between 50 and 150 m.

The Coastal Ocean Model

We used a coastal ocean model system consisting of a North Sea model with 20-km horizontal grid resolution and a Western Norwegian coast model with 4-km horizontal resolution nested in the North Sea model to model explicitly the open boundary conditions toward the coast for the fjord model. The Princeton Ocean Model (Blumberg and Mellor 1987) is the main engine for the implementation of both the North Sea model and the Western Norwegian coast model. The Princeton Ocean Model is a primitive-equation, free-surface, three-dimensional, σ-coordinate ocean model. This model has been used for many years at the Institute of Marine Research and is named the Norwegian Ecological Model System (NORWECOM; Skogen and Søiland 1998). Initial values as well as boundary conditions for the North Sea model were taken from climatologies (Martinsen et al. 1992). The model system was forced by atmospheric fields from the hindcast archive of the Norwegian Meteorological Institute (Reistad and Iden 1998) and river data from a multitude of sources. Boundary values for the fjord model were written every 30 minutes.

The Atmospheric Model

The MM5 mesoscale atmospheric model is a nonhydrostatic σ-coordinate model developed at the Pennsylvania State University and the National Center for Atmospheric Research in the United States (Dudhia 1993). For the present study, MM5 was configured with two domains with horizontal grid resolutions of 9 km and 3 km. The innermost nest covered the western part of Norway including both the Sognefjord and the Hardangerfjord. In the vertical, 23 σ-coordinates were used where the lower level was approximately 38 m above the surface and the upper level at 15-km height. The MM5 contains parameterizations and submodels for turbulence, radiation, and cloud physics. Initial conditions were taken from the analyzed atmospheric fields of the European Centre for Medium Range Weather Forecasts, as well as boundary conditions every 6 hours. Results from the MM5 model were interpolated onto the fjord model grid as 6 hourly snapshot values.

The Fjord Model

The Bergen Ocean Model is a three-dimensional σ-coordinate numerical model solving the so-called primitive equations (i.e., conservation of momentum, mass, salt, and temperature). The Bergen Ocean Model is developed at the University of Bergen and the Institute of Marine Research by Berntsen et al. (1996) on the basis of the Princeton Ocean Model. The prognostic variables are three-dimensional current, hydrography, water level, turbulent length scale, and turbulent kinetic energy. The Bergen Ocean Model has an embedded turbulence model (Mellor and Yamada 1982). The equations were solved using finite difference techniques on a staggered Arakawa C-grid. The time step was explicit. For the fjords in western Norway, the Cartesian horizontal grid consisted of 800×800 m^2 (Figure 1.4). In the vertical, 21 levels were used with the highest resolution in the upper few meters where grid cells can only be a few

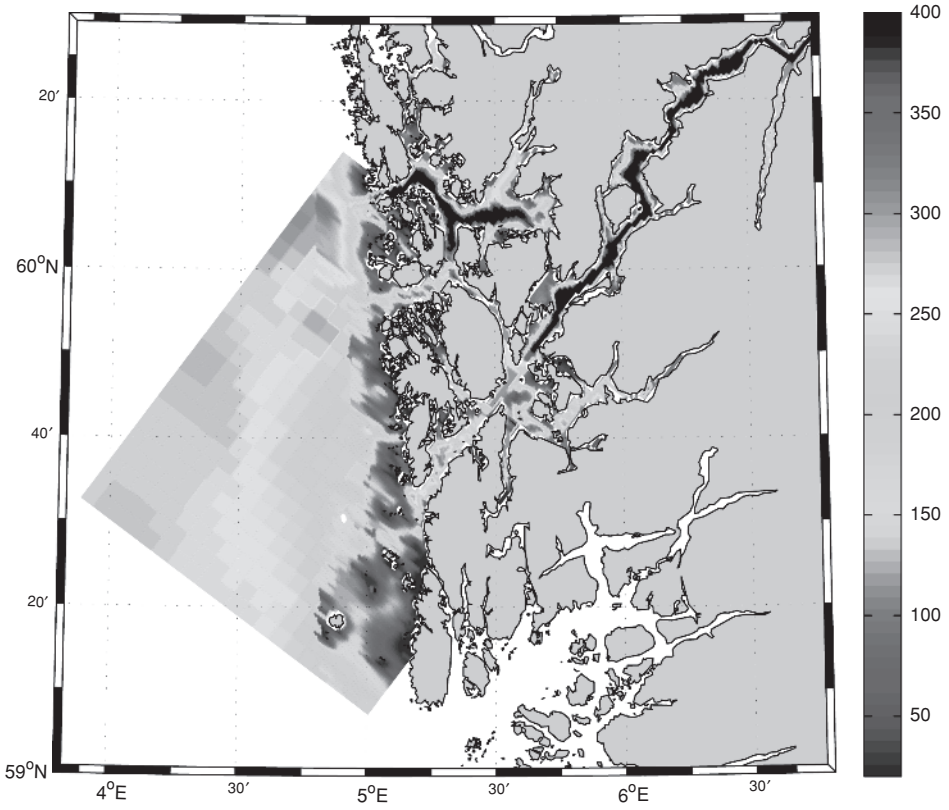

Figure 1.4. The orientation and bottom depths for the Hardangerfjord numerical fjord model grid with an 800-m horizontal resolution. (See also color plate section.)

decimeters deep in order to resolve vertical gradients caused by wind and freshwater runoff. Maximum depth was set to 400 m for technical reasons, but this will not critically affect the results for the upper 50 m, which is the region of interest for salmon lice. The details of the bottom topography below 400 m will only slightly affect the phase velocity of the tides (Asplin et al. 1999). The initial model values contained static stable conditions without any flow or water elevation and a typical vertical stratification for the simulated period. Every 30 minutes, the values at the open boundary were updated from the results of the coastal model using a flow relaxation scheme—boundary condition (Martinsen and Engedahl 1987). Every 6 hours, the wind forcing was updated from the MM5 model. River runoff was included from 62 separate rivers, on the basis of a few measurements and/or interpolations from the Norwegian Water Resources and Energy Directorate and Statkraft.

The Salmon Lice Growth and Advection Model

The growth and advection in three dimensions of the first three planktonic stages of salmon lice have been modeled. The tricky part of this modeling is to incorporate

the lice behavior, which is virtually impossible to observe other than in controlled laboratory experiments. Such models have been developed by Gillibrand and Willis (2007), Gillibrand and Amundrud (2007), and Amundrud and Murray (2007). Water current advection of salmon lice was measured using a standard particle-transport model with hourly current values from the fjord model and a random walk diffusion (Ådlandsvik and Sundby 1994). At each 6-minute step, the particles were given an axisymmetric Gaussian random velocity. Typically, a diffusion coefficient in the range 1–10 $m^2\ s^{-1}$ was used. For this advectional part of the salmon lice model, the quality of the fjord current model is believed to be most critical.

For the growth of the salmon louse, we used empirical data from laboratory experiments (Boxaspen, unpublished data) and numbers reported by Stien et al. (2005). These results indicated that the salmon louse copepodid was infectious between 50 and 150 degree days after hatching. Salmon lice behavior in the model is based on the following assumptions:

(1) The salmon louse has a diel migration, i.e., it swims toward the surface during daytime and downward during nighttime (Heuch et al. 1995; Hevrøy et al. 2003).
(2) Salmon lice are limited to depths above 10 m since this is where wild salmon smolts reside (Davidsen et al. 2008).
(3) Salmon lice avoid water of salinity <20 by swimming downward (Heuch 1995).

By excluding salmon lice below 10-m depth, we only model the proportion of the planktonic population with the best chance to encounter a wild salmon smolt. The quality of the salmon lice growth and advection model might be improved by improving the louse behavior, although we need to model the mean behavior of "super particles," i.e., model particles representing a large number or certain representative or only the successful lice.

Model Results of the Distribution and Abundance of Planktonic Salmon Lice

We present examples from the variable environmental conditions and salmon lice distribution supporting the following general features of planktonic salmon lice found in Norwegian waters

(1) Planktonic salmon lice can spread quickly.
(2) Salmon lice can spread over large areas, although the majority of the salmon lice generally do not move very far from a given source.
(3) The variability of salmon lice spreading is large.

Results that we have gathered during recent years from different locations in Norwegian fjords and coastal waters indicate that the distribution and abundance of planktonic salmon lice vary substantially in a relatively unpredictable manner. This variability is related to high variability of fjord environmental conditions. Most of our sample results are from the fjords in the western part of Norway (the Hardangerfjord and the Sognefjord), but the results can typically be generalized to any fjord area along the Norwegian coast.

Variability of the Fjord Hydrography

The time variability of the hydrography in the surface waters of a fjord spans from a few hours up to seasonal and interannual scales. Temperature measurements from the observational buoy in the Hardangerfjord (its position is marked by "buoy" in Figure 1.2) at 3-m depth between July and December 2008 illustrate this variability (Figure 1.5). The seasonal signal is obvious with a high summer value and a gradual cooling through the fall. Superimposed on this trend are fluctuations of many periods and some with large amplitudes. These measurements are from the main fjord, and horizontal advection of water of different temperature is likely to occur. Frequent episodes of wind mixing the water both horizontally and vertically also occur. Thus, the temperature variability might be less in more sheltered areas such as in smaller fjords and fjord arms. We found that a change in temperature of 2–4°C can happen within days, e.g., around day 220 or 330 (Figure 1.5).

Variability of salinity in the surface waters is associated with the variability of temperature. The lowest salinity values are in the summer, and a gradual increase occurs during the fall as illustrated from the Hardangerfjord buoy measurements at 3-m depth in June to December 2008 (Figure 1.6). Variable runoff, as well as episodes of strong winds and horizontal advection of water masses of different salinity, produces occasionally large fluctuations in the long term. Oscillations produced by internal waves occur because the density of the cooler water is mostly determined by salinity. As long as the salinity is higher than 20, its variability in the surface layer will probably not affect the salmon lice, other than the inhibiting effect of the pycnocline to vertical motion and the vertical swimming of the salmon lice. Rapid changes in salinity can occur within only a few days, e.g., around day 220 with an increase of 4–5 and around day 300 with a drop of 5–6 (Figure 1.6). In the summer period, between day 190 and 240, large oscillations of a short duration appear. This is probably when the vertical position of the halocline is in the proximity of the sensor

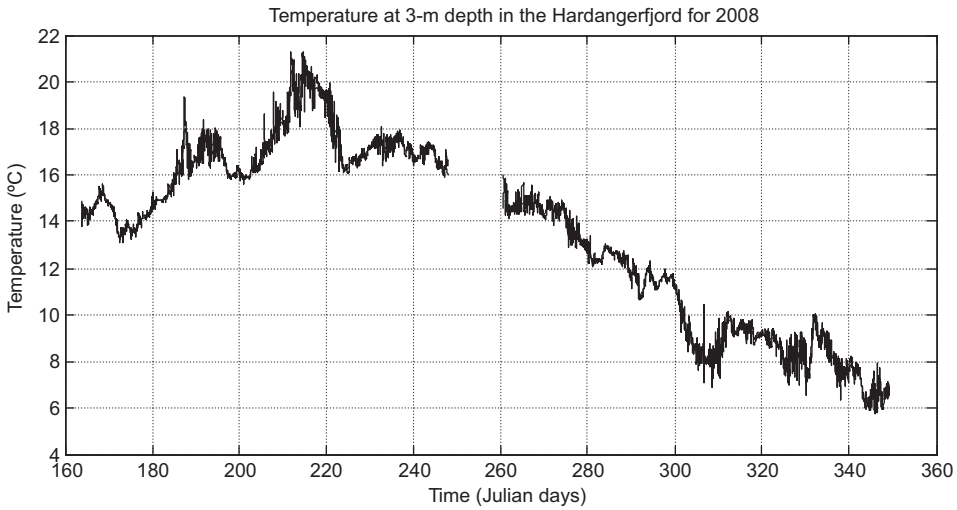

Figure 1.5. Time series of temperature (°C) at 3-m depth from the Hardangerfjord buoy as 10-minute measurements from June to December 2008.

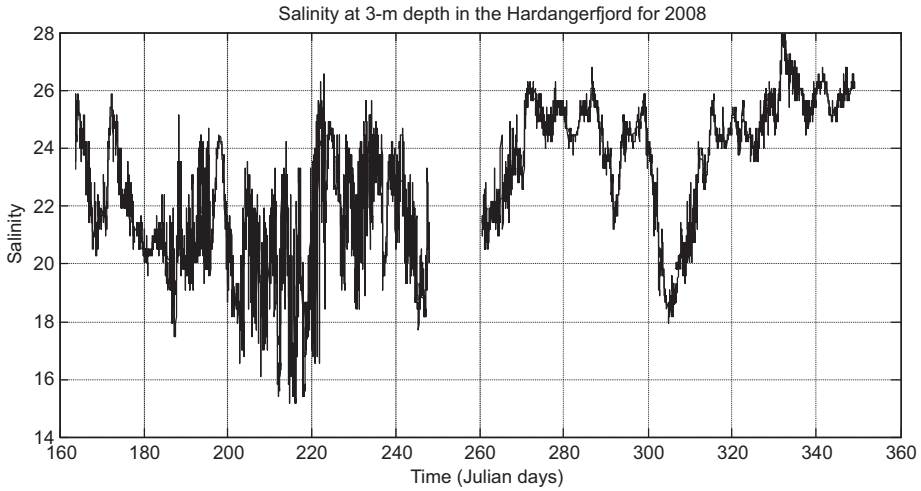

Figure 1.6. Time series of salinity at 3-m depth from the Hardangerfjord buoy as 10-minute measurements from June to December 2008.

(at 3-m depth) and only small vertical shifts of water create large variations in the measured salinity.

Because of interannual differences in regional precipitation and melting conditions, the horizontal extension of the brackish layer in the fjords will also vary interannually. We found large variations of the brackish water horizontal extension in the Hardangerfjord for June 2004–2010 (Figure 1.7). The thickness of the brackish layer was similar between the years, approximately 5–10 m, but the salinity varied significantly. The year of lowest salinity was 2005 with values <15–20 outside the fjord. The highest salinities of the brackish layer occurred in 2004, 2006, and 2009 when the measured values were mostly above 20. The horizontal extent of the brackish layer varies as well. Using a salinity of 25 as a measure, we found this isohaline farthest out of the fjord in 2007, followed by the years 2005 and 2008 with a brackish layer extension far out of the fjord. In 2004, 2006, and 2010, the horizontal extension of the measured brackish layer in June was much shorter and 50–80 km less than that for 2007 (Figure 1.7).

Variability of the Fjord Current

Many factors affect the variability of the currents within a fjord. The brackish layer flow is typically strongest during the spring and summer when river runoff is at its highest. The wind-driven flow is usually stronger during the winter, although strong local wind episodes can occur year round. The tides vary between spring and neap phase, and the tidal wave propagating into the fjord from a water level change at the mouth will create stronger currents in areas of narrow and restricted topography (Farmer and Freeland 1983). In other seasons, the tidal flow inside the fjords is usually modest as it often will be part of a standing wave. The stratification of the water masses in the coastal water outside the fjords can produce internal pressure gradients into the fjords and create internal waves in wide fjords, i.e., larger than 2–3 km (Asplin et al.

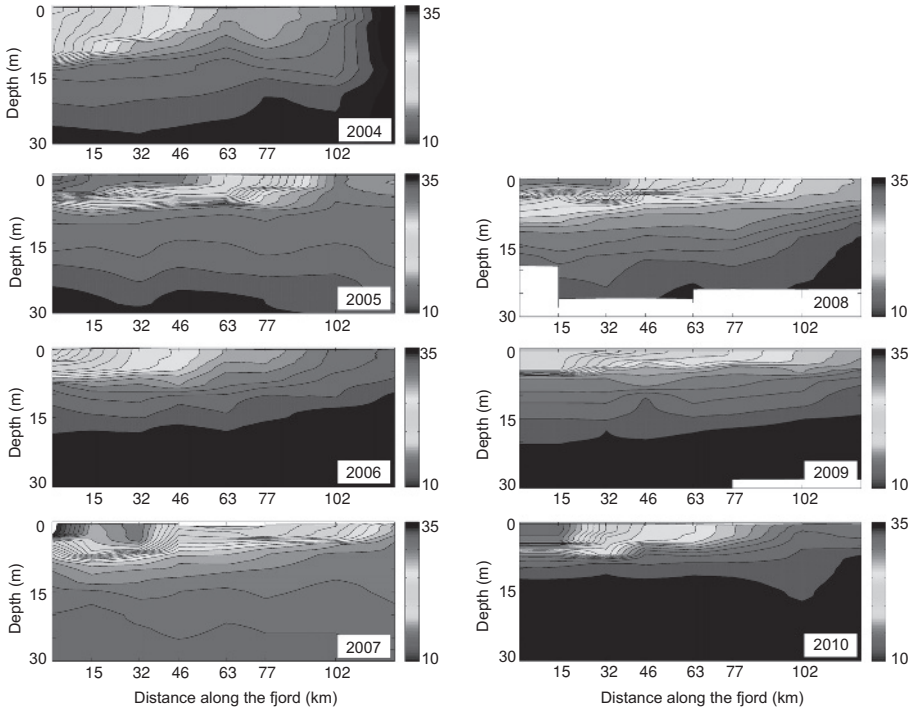

Figure 1.7. Vertical long sections of salinity in June for the years 2004–2010 showing the interannual difference in the extension of the brackish water layer. The fjord head is to the left and the mouth to the right in the figures. The location of the section corresponds to the red line in the map of Figure 1.2. (See also color plate section.)

1999; Sundfjord 2010). These waves propagate at a modest speed of 0.5–1 m s^{-1} and can last for several days. The associated current, which can be directed both into and out of the fjord, can move large amounts of water in the upper 50–100 m of the fjords.

As an illustration of currents in a large fjord, measurements from the buoy in the Hardangerfjord at 11-m depth for the period June–December 2008 showed significant fluctuations in velocity (Figure 1.8). The buoy position is marked in Figure 1.2. The flow component along the fjord axis is shown, and mean values exceeded 0.5 m s^{-1} on several occasions. The measurements identify a modest tidal flow of less than 0.1 m s^{-1} of amplitude, which is to be expected at this location where the fjord is several kilometers wide and more than 500 m deep. Other variability included rapid episodes of a strong current lasting for only a few days, probably due to strong winds (single peaks, e.g., around day 170 or 330) and episodes of relatively high mean currents lasting for many days, probably induced by internal waves propagating into the fjord from the coast (e.g., between day 180 and 200).

Fjord Model Current Validation

A good representation of the current and current dispersion is important for the fjord model of salmon lice advection. In April–May 2007, there was a reasonable

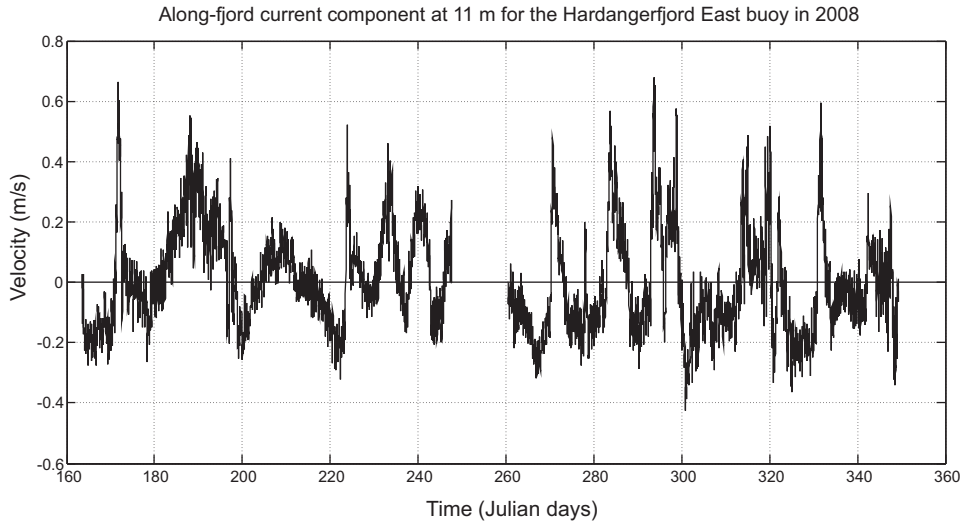

Figure 1.8. Time series of along-fjord current (m s^{-1}) at 11-m depth from the Hardangerfjord buoy as 10-minute measurements from June to December 2008. Positive values are shown into the fjord.

comparison between the numerical model results and a central current observation. The current measurement was taken farther out of the fjord (at the position marked "mooring" on Figure 1.2), and the daily mean values at 5-m depth describe a typical period of shifting conditions and large episodes of inflow or outflow to the fjord, each lasting several days (Figure 1.9). The observation is compared with the numerical model results for the same period (red line). Obviously, the fit between the observed and modeled current is not perfect, but the results are sufficient to confidently force

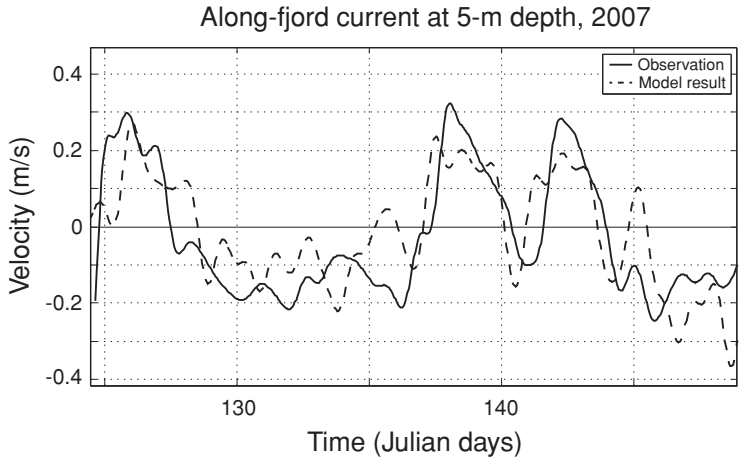

Figure 1.9. Time series of along-fjord current (m s^{-1}) at 5-m depth from the Nortek Aquadopp profiler as 24 hours low-passed values from May 2007. Positive values are shown into the fjord. The red line is comparable values from results of the fjord model.

Table 1.1. Statistics of the numerical model results and the current meter mooring at the position in the middle of the Hardangerfjord in May 2007. The currents are along the main fjord axis decomposed onto inward and outward directions.

Mooring	Depth (m)	Mean current inward (m s^{-1})	SD current inward (m s^{-1})	Mean current outward (m s^{-1})	SD current outward (m s^{-1})
Fjord model	10	0.21	0.14	0.22	0.13
Current mooring	10	0.23	0.16	0.17	0.12
Fjord model	30	0.14	0.10	0.19	0.10
Current mooring	30	0.17	0.11	0.13	0.09

the salmon lice growth and advection model with the model current. Looking closer at the numbers, it is possible to identify a reasonable match between mean flow and the standard deviation when separating the current into inward and outward flow (Table 1.1).

Results of the Salmon Lice Model

Spread Quickly

The salmon lice model shows that salmon lice can spread quickly within the fjord. This depends on the variable current in the fjord, and the spread will be slow if released in a period of slack current. An example of rapid and rather unpredictable spreading of salmon lice is given in the results of a model simulation from May 2007 (i.e., from a period where the fjord model current compares favorable with observations, as shown in the section "Fjord Model Current Validation"). Only 24 hours are simulated using the salmon lice growth and advection model and realistic currents from the fjord model. Three batches of 200 model lice were released on May 1, May 5, and May 10, respectively (Figure 1.10). After 12 hours, the model salmon lice in the three batches were localized relatively close, but the batches did not overlap. Twelve hours later, the batch of May 5 (green colored) moved approximately 30 km into the fjord, which corresponded to a speed of 0.7 m s^{-1}. This is considered rapid, but according to the current observations, such current speeds are not unrealistic for shorter periods. The batch released on May 1 (red colored) moved 20 km out of the fjord between 12 and 24 hours corresponding to a speed of almost 0.5 m s^{-1}. The model salmon lice of the batch released on May 10 (blue colored) were no longer localized together but had spread out in most of the outer fjord system. This occurred during only 12 hours, and the speed of the individual salmon lice ranged from zero to more than 1 m s^{-1}.

Spread over Large Areas

Another important result is that during their lifespan (up to about 150 degree days, typically 2–3 weeks for water temperatures in the range 7–14°C), salmon lice can spread over a large area. This is illustrated by two model simulations, which only differ in how the salmon lice were released. Both simulations were from April 29 to May 18

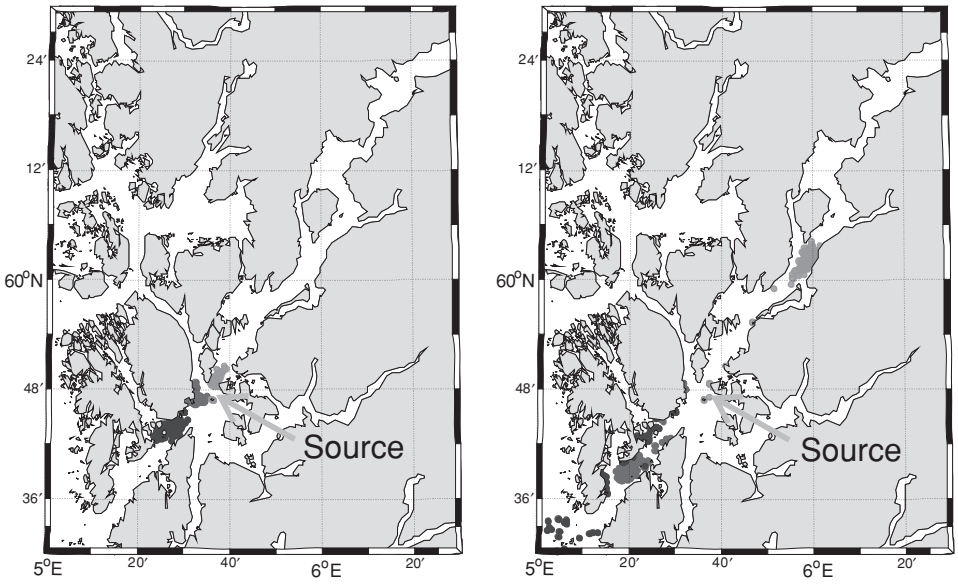

Figure 1.10. Modeled spreading of salmon lice from a single source (blue arrow) and from three different release dates. Results after 12 hours (left panel) and 24 hours (right panel) are shown. The red-colored salmon lice were released on May 1, the green-colored salmon lice were released on May 5, and the blue-colored salmon lice were released on May 10, 2007. (See also color plate section.)

in 2007. A total of 800 model salmon lice were released for both simulations from only one source. For the first simulation, all 800 model salmon lice were released at the start on April 29. For the second simulation, 5 model lice were released every 3 hours throughout the period. The results from both simulations showed a distribution over a large area, covering most of the fjord system (Figure 1.11). The two different ways of releasing model salmon lice apparently do not influence the distribution in a significant manner. The distribution of the maximum distance traveled by the individual model salmon louse for a 10-day period in May 2007 showed that most of the salmon lice did not move very far from the source, i.e., typically less than 25 km (Figure 1.12). However, we did find a small number of salmon lice were able to travel more than 200 km in this 10-day period.

Large Variability

The variability of planktonic salmon lice distribution depends mostly on the variable number of hatched eggs and variability of the currents. The salmon lice advection model can only quantify the variability of the currents, as the number of salmon lice modeled must be specified a priori. The currents vary in the range from hours up to interannually, and we expected to find that the variability of the salmon lice spreading is a reflection of the scale of current variability.

We have seen in the previous model example that a batch of model salmon lice released only 5 days prior to another moved in a totally different direction (Figure 1.10). This serves as an example of the variability of spreading on a short time scale (hours).

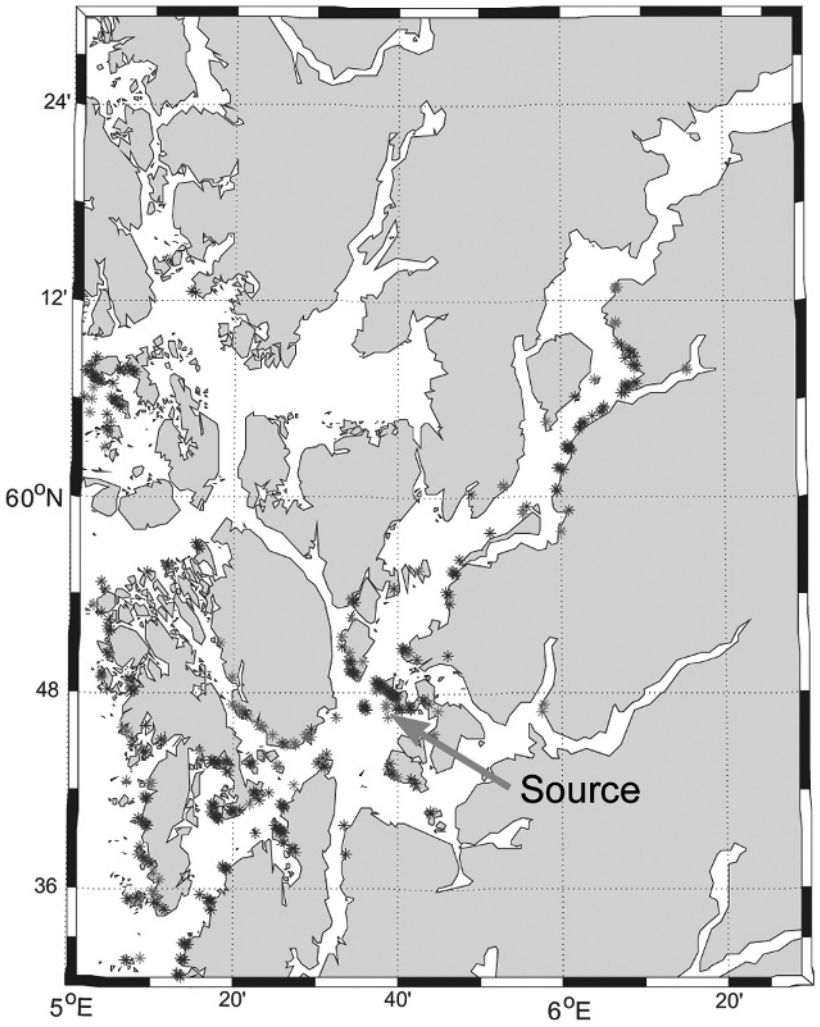

Figure 1.11. Modeled spreading of salmon lice from a single source and from two different experiments. Results at the end of the simulated period between April 29 and May 18, 2007, are shown. The blue-colored lice correspond to a simulation with a batch of 800 lice released at the start of the simulation and the red-colored model lice correspond to a simulation where 5 lice are released every 3 hours for the whole period. (See also color plate section.)

By performing sufficient model experiments, it is possible to illustrate variability on many time scales.

An example of interannual variability of salmon lice distribution is from the outer part of the Sognefjord where we measured the distribution of planktonic salmon lice from an array of sentinel cages in May 2001 and May 2003. We modeled salmon lice distribution for the same periods (Figure 1.13). Both the distribution from the observations and the model results indicate that in May 2001 salmon lice spread into the fjord and in 2003 the spreading was out of the fjord and to the north. The only difference in the model results from 2001 and 2003 is the environmental conditions

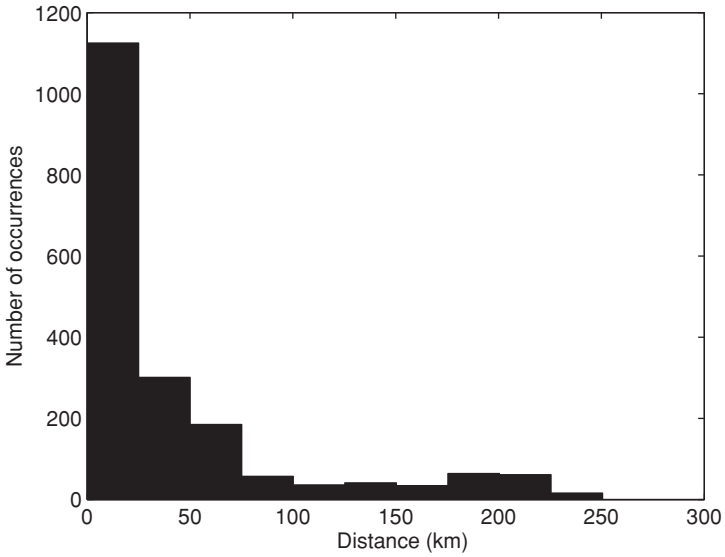

Figure 1.12. Distribution of the distance traveled in 10 days for salmon lice particles from the release position marked by source in Figure 1.11.

(the number and release of the salmon lice are identical), and the reason for the different distribution is the integrated effect of the current variability over the simulated period (May 8–28). The mean wind vector clearly indicates a more inward current system in 2001 compared to 2003. The difference in abundance (10 times more lice in 2001 than in 2003) cannot be explained by environmental variability. This can only be due to the number of hatched eggs produced between the 2 years. There were either fewer salmon farms in operation in 2003 compared to 2001 or the farmers improved their delousing skills.

Concluding Remarks

The variation in the distribution of the planktonic salmon lice relates directly to the environmental variability. This variability is from hours to years and from hundreds of meters to the fjord scale. Variable currents will affect the distribution of the planktonic salmon lice, possibly moving them more than 100 km from their source (although the majority of the salmon lice move much less). Water temperature has an important influence on the growth of the salmon louse and the evolution of their populations. Salmon lice growth and egg hatching times are particularly sensitive in the temperature range between 5 and 15°C, temperatures typical of the spring in Norwegian fjords.

It will be of crucial importance to be able to quantify the effects of environmental variability on the abundance and distribution of planktonic salmon lice. This will necessarily be related to the production of salmon lice for a region. Other factors, and possibly more important for such an estimate, will be the number and size of the fish as well as the delousing treatment success for a salmon lice population on farmed fish.

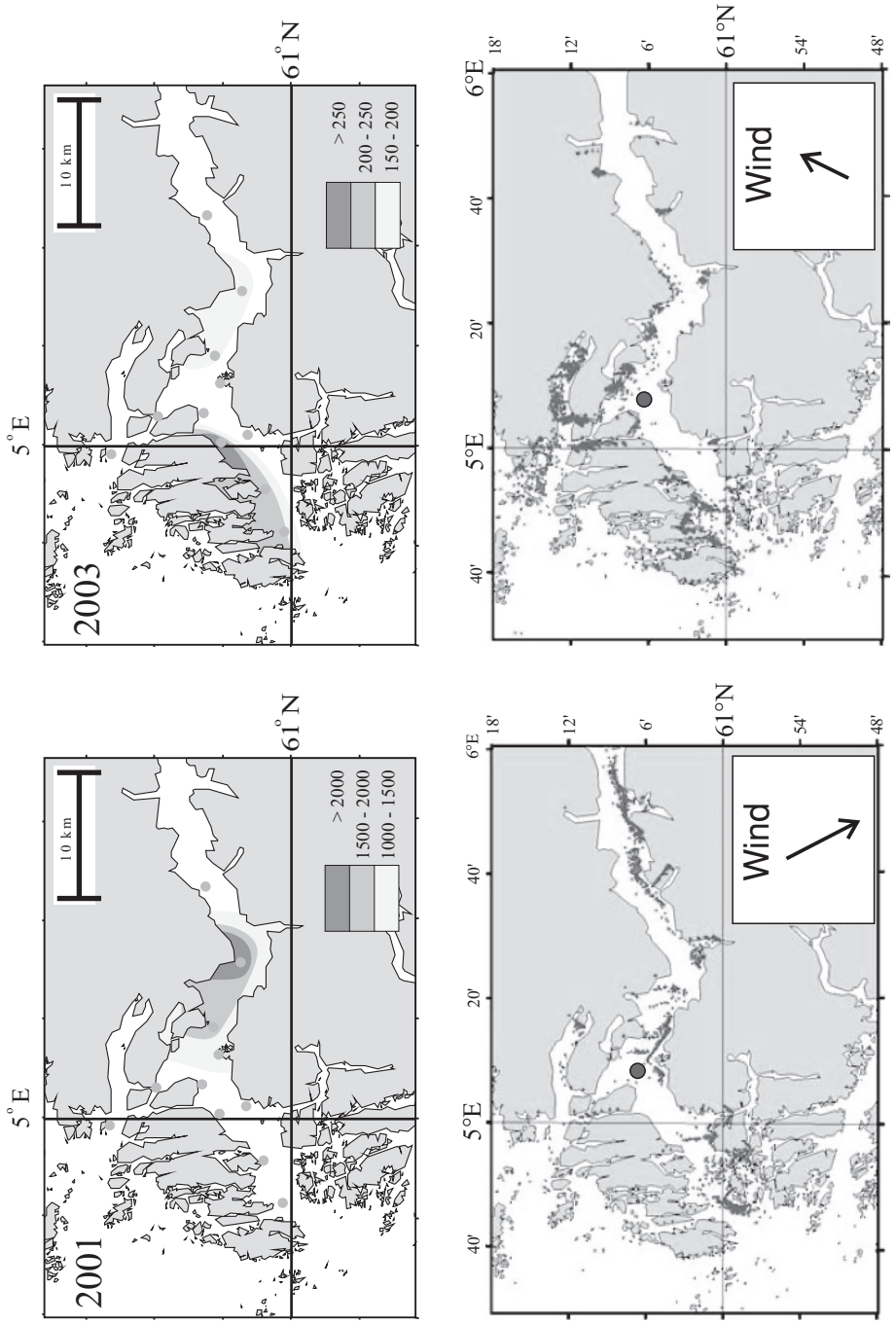

Figure 1.13. Observations of salmon lice distribution and abundance from sentinel cages in the spring of 2001 and 2003 (upper panels) and salmon lice model results for the same period (lower panels). Blue dots in the upper panels show the positions of the cages. The large red dots in the lower panels mark the release position for the model salmon lice. The wind vectors represent the average wind for the simulated period May 8–28 in 2001 and 2003, respectively. (See also color plate section.)

An approach using a population dynamics model for salmon lice coupled to an advection and growth model might quantify the appropriate capacity of a region to contain salmon lice from aquaculture. Maintaining aquaculture and the sea trout stocks residing within fjords is challenging from the management standpoint. A modeling approach will possibly be a way to manage fish farms such that there will be capacity for both the wild fish and an aquaculture industry.

References

Ådlandsvik, B. and Sundby, S. 1994. Modelling the transport of cod larvae from the Lofoten area. *ICES Journal of Marine Science Symposium* **198**: 379–392.

Amundrud, T.L. and Murray, A.G. 2007. Validating particle tracking models of sea lice dispersion in Scottish sea lochs. *ICES CM 2007*/B:05,12 p.

Asplin, L., Salvanes, A.G.V., and Kristoffersen, J.B. 1999. Non-local wind-driven fjord-coast advection and its potential effect on plankton and fish recruitment. *Fisheries Oceanography* **8**: 255–263.

Berntsen, J., Skogen, M.D., and Espelid, T.O. 1996. Description of a sigma-coordinate ocean model. *Fisken og havet*, Institute of Marine Research, Norway, **12**, 33 p.

Blumberg, A.F. and Mellor, G.L. 1987. A description of a three-dimensional coastal ocean circulation model. In: *Three-Dimensional Coastal Ocean Models* (ed. N. Heaps), Vol. 4, pp. 1–16. American Geophysical Union, Washington, DC.

Davidsen, J.G., Plantalech Manel-la, N., Økland, F., Diserud, O.H., Thorstad, E.B., Finstad, B., Sivertsgård, R., McKinley, R.S., and Rikardsen, A.H. 2008. Changes in swimming depths of Atlantic salmon *Salmo salar* post-smolts relative to light intensity. *Journal of Fish Biology* **73**: 1065–1074.

Dee, D.P. 1995. A pragmatic approach to model validation. In: *Quantitative Skill Assessment for Coastal Ocean Models* (eds D.R. Lynch and A.M. Davies), pp. 1–13. American Geophysical Union, Washington, DC.

Dudhia, J. 1993. A nonhydrostatic version of the Penn State-NCAR mesoscale model: validation tests and simulation of an Atlantic cyclone and cold front. *Monthly Weather Review* **121**: 1493–1513.

Dyer, K.R. 1997. Estuaries*:* A Physical Introduction. John Wiley & Sons, Ltd., Chichester, 195 p.

Farmer, D.M. and Freeland, H.J. 1983. The physical oceanography of fjords. *Progress in Oceanography* **12**(2): 147–220.

Gillibrand, P.A. and Amundrud, T.L. 2007. A numerical study of the tidal circulation and buoyancy effects in a Scottish fjord. *Journal of Geophysical Research (Oceans)* **112**: C05030.

Gillibrand, P.A. and Willis K. 2007. Dispersal of sea louse larvae from salmon farms: modelling the influence of environmental conditions and larval behaviour. *Aquatic Biology* **1**: 63–75.

Hansen, L.P., Fiske, P., Holm, M., Jensen, A.J., and Sægrov, H. 2008. Bestandsstatus for laks i Norge. Prognoser for 2008. Rapport fra arbeidsgruppe. Utredning for DN 2008-5, 66 p. (In Norwegian.)

Heuch, P.A. 1995. Experimental evidence for aggregation of salmon louse copepodids, *Lepeophtheirus salmonis*, in step salinity gradients. *Journal of the Marine Biological Association of the United Kingdom* **75**: 927–939.

Heuch, P.A., Bjørn, P.A., Finstad, B., Holst, J.C., Asplin, L., and Nilsen, F. 2005. A review of the Norwegian National Action Plan Against Salmon Lice on Salmonids: the effect on wild salmonids. *Aquaculture* **246**: 79–92.

Heuch, P.A., Parsons, A., and Boxaspen, K. 1995. Diel vertical migration: a possible host-finding mechanism in salmon louse (*Lepeophtheirus salmonis*) copepodids? *Canadian Journal of Fisheries and Aquatic Sciences* **52**: 681–689.

Hevrøy, E.M., Boxaspen, K.K., Oppedal, F., Taranger, G.L., and Holm, J.C. 2003. The effect of artificial light treatment and depth on the infestation of the sea louse *Lepeophtheirus salmonis* on Atlantic salmon (*Salmo salar* L.) culture. *Aquaculture* **220**: 1–14.

Martinsen, E.A. and Engedahl, H. 1987. Implementation and testing of a lateral boundary scheme as an open boundary condition for a barotropic model. *Coastal Engineering* **11**: 603–637.

Martinsen, E.A., Engedahl, H., Ottersen, G., Ådlandsvik, B., Loeng, H., and Baliño, B. 1992. MetOcean MOdeling Project, Climatological and hydrographical data for hindcast of ocean currents. Technical report 100. The Norwegian Meteorological Institute, Oslo, Norway, 93 p.

Mellor, G.L. and Yamada, T. 1982. Development of a turbulence closure model for geophysical fluid problems. *Reviews of Geophysics and Space Physics* **20**: 851–875.

Penston, M.J., McKibben, M.A., Hay, D.W., and Gillibrand, P.A. 2004. Observations on open-water densities of sea lice larvae in Loch Shieldaig, Western Scotland. *Aquaculture Research* **35**: 793–805.

Reistad, M. and Iden, K.A. 1998. Updating, correction and evaluation of a hindcast data base of air pressure, winds and waves for the North Sea, Norwegian Sea and the Barents Sea. Technical report 9. Det Norske Meteorologiske Institutt, Oslo, Norway, 42 p.

Skogen, M.D. and Søiland, H. 1998. A user's guide to NORWECOM v2.0. The NORWegian ECOlogical Model system. Technical report. *Fisken og havet* 18/98, Institute of Marine Research, Pb. 1870, N-5024 Bergen, Norway, 42 p.

Stien, A., Bjorn, P.A., Heuch, P.A., and Elston, D.A. 2005. Population dynamics of salmon lice *Lepeophtheirus salmonis* on Atlantic salmon and sea trout. *Marine Ecology Progress Series*, **290**: 263–275.

Sundfjord, V.N. 2010. Volume transport due to coastal wind-driven internal pulses in the Hardangerfjord. Master's thesis, Department of Geosciences, MetOs section, University of Oslo, Norway, 62 p.